A Game Theoretic Approach to Risk-Based Optimal Bidding Strategies for Electric Vehicle Aggregators in Electricity Markets With Variable Wind Energy Resources

Hongyu Wu, *Member, IEEE*, Mohammad Shahidehpour, *Fellow, IEEE*,
Ahmed Alabdulwahab, *Senior Member, IEEE*, and Abdullah Abusorrah, *Senior Member, IEEE*

***Abstract*—This paper proposes a stochastic optimization model for optimal bidding strategies of electric vehicle (EV) aggregators in day-ahead energy and ancillary services markets with variable wind energy. The forecast errors of EV fleet characteristics, hourly loads, and wind energy as well as random outages of generating units and transmission lines are considered as potential uncertainties, which are represented by scenarios in the Monte Carlo Simulation (MCS). The conditional value at risk (CVaR) index is utilized for measuring EV aggregators' risks caused by the uncertainties. The EV aggregator's optimal bidding strategy is formulated as a mathematical programming with equilibrium constraints (MPEC), in which the upper level problem is the aggregators' CVaR maximization while the lower level problem corresponds to the system operation cost minimization. The bi-level problem is transformed into a single-level mixed integer linear programming (MILP) problem using the prime-dual formulation with linearized constraints. The progressive hedging algorithm (PHA) is utilized to solve the resulting single-level MILP problem. A game theoretic approach is developed for analyzing the competition among the EV aggregators. Numerical cases are studied for a modified 6-bus system and the IEEE 118-bus system. The results show the validity of the proposed approach and the impact of the aggregator's bidding strategies on the stochastic electricity market operation.**

***Index Terms*—Electric vehicle aggregators, strategic bidding, wind energy, conditional value at risk (CVaR), incomplete information, Nash equilibrium.**

NOMENCLATURE

Indices

n Index for aggregators.
t Index for time periods.
i Index for thermal generating units.
c Index for EV fleets.
d Index for buses.
k Index for wind generators.
m Index for blocks of thermal unit dispatch.
s Index for base case $s = 0$ and scenarios.

Sets and Signs

Θ_n	Set of EV fleets controlled by aggregator n.
TP_n	Set of types of EV aggregator.
Q, NQ	Set of quick-start/non-quick-start thermal generating units.
T_c	Set of flexible charging periods for EV fleet c
$\overline{(\cdot)}$	Given (input) variables.

Parameters

NT	Number of time periods.
NG	Number of thermal generating units.
NK	Number of wind generators.
NL	Number of transmission lines.
NS	Number of scenarios.
NA	Number of aggregators.
NM	Number of blocks of thermal unit dispatch.
$P_c^{\max}$	Maximum charging power of EV fleet c, in MW.
$SOC_c^{\max}, SOC_c^{\min}$	Max/min SOC of EV fleet c, in MWh.
$E_{n,t}^{\max}, E_{n,t}^{\min}$	Max/min total charging energy of aggregator n at time t, in MWh.
$PG_i^{\max}, PG_i^{\min}$	Max/min power generation of unit i, in MW.
$RU_i^{\max}, RD_i^{\max}$	Maximum ramp up/down rate of thermal unit i, in MW/hour.
$CREQ_c$	Charging requirement for EV fleet c, in MWh.
REQ_t^{UP}, REQ_t^{DN}	System up/down reserve requirement at time t, in MW.
QSC_i	Quick-start capacity of thermal unit i, in MW.
$I_{i,t}^s$	State of thermal generating unit i at time t; 1 for ON and 0 for OFF.
$\mu_{m,i,t}$	Marginal production cost (bidding price) of the *m-th* block of unit i at time t, in \$/MW.

Manuscript received January 27, 2014; revised August 18, 2014, April 22, 2015, and July 25, 2015; accepted July 30, 2015. Date of publication December 08, 2015; date of current version December 11, 2015. This work was supported by the National Science, Technology, and Innovation Plan Strategic Technologies Program in the Kingdom of Saudi Arabia under Project Grant 12-ENE3194-03. Paper no. TSTE-00038-2014.

H. Wu is with the Power Systems Engineering Center, National Renewable Energy Laboratory, Golden, CO 80401 USA (e-mail: hongyu.wu@nrel.gov).

M. Shahidehpour is with the Robert W. Galvin Center for Electricity Innovation, Illinois Institute of Technology, Chicago, IL 60616 USA, and also with the Department of Electrical and Computer Engineering, King Abdulaziz University, Jeddah 21589, Saudi Arabia (e-mail: ms@iit.edu).

A. Alabdulwahab and A. Abusorrah are with the Renewable Energy Research Group, Department of Electrical and Computer Engineering, King Abdulaziz University, Jeddah 21589, Saudi Arabia.

Color versions of one or more of the figures in this paper are available online at http://ieeexplore.ieee.org.

Digital Object Identifier 10.1109/TSTE.2015.2498200

NL_i No-load cost of thermal unit i, in \$.
β Share of revenue from offering the regulation service, in %.
η Charging efficiency, in %.
$\Pr^s$ Probability of scenario s
$\Pr(\cdot)$ Probability of bidding strategy.
τ Time interval, 1 hour.
α Confidence (risk) level.
M Sufficiently large constant.
$\varphi_1, \varphi_2, \phi_1, \phi_2$ Coefficients of linear regression.

Variables

$LMP^s_{c,t}$ Locational marginal price for EV fleet c at time t in scenario s, in \$/MWh.
$\lambda^{UP}_{c,t}, \lambda^{DN}_{c,t}$ Up/down regulation price for EV fleet c at time t, in \$/MW.
$\Delta\gamma_{n,t}$ Energy price markup (bidding strategy) for aggregator n at time t, in \$/MWh.
$E^s_{c,t}$ Awarded energy bid for EV fleet c at time t in scenario s, in MWh.
$\Delta E^s_{c,t}$ Energy deviation between day-ahead and real-time markets for EV fleet c at time t in scenario s, MWh.
$R^{UP}_{c,t}, R^{DN}_{c,t}$ Awarded up/down regulation offer (quantity) for EV fleet c at time t, in MW.
$RG^{UP}_{i,t}, RG^{DN}_{i,t}$ Awarded up/down regulation offer for thermal generator i at time t, in MW.
$P^s_{c,t}$ Preferred operating point (POP) for EV fleet c at time t in scenario s, in MW.
$PA^s_{n,t}$ Aggregated charging power for aggregator n at time t in scenario s, in MW.
$PG^s_{i,t}$ Dispatch of thermal generating unit i at time t in scenario s, in MW.
$\Delta PG^s_{i,t}$ Dispatch deviation between the day-ahead and real-time markets for thermal unit i at time t in scenario s, in MW.
$SOC^s_{c,t}$ State of charge (available battery energy) for EV fleet c at time t in scenario s, in MWh.
$PR^s_{k,t}$ Dispatch of wind generator k at time t in scenario s, in MW.
$SU^s_{i,t}, SD^s_{i,t}$ Startup/shutdown cost of unit i at time t in scenario s, in \$.
EP^s_n Payoff of aggregator n in scenario s, in \$.
$FT^s_{i,t}$ Transition cost of quick-start unit i at time t in scenario s, in \$.

Random Numbers

$G^{f,s}_{k,t}$ Available generation of wind generator k at time t in scenario s, in MW.
$PD^s_{d,t}$ Hourly load of bus d at time t in scenario s, in MW.

Matrices and Vectors

$\mathbf{SF}$ Shift factor matrix.
$\mathbf{PL^{max}}$ Vector of upper limit for power flow.
$\mathbf{K_P}, \mathbf{K_D}$ Bus-generator/bus-load incidence matrix.
$\mathbf{P^s}$ Vector of generation dispatch in scenario s with the dimension of $(NG + NK) \times NT$.

I. Introduction

THE QUEST for the electrification of vehicles is heralded as one of the important alternatives to the reduction of greenhouse gas emissions and fossil fuel consumptions. Electric vehicles (EVs) offer numerous advantages over traditional vehicles with internal combustion engines, which include lower operating costs and higher potentials for utilizing locally generated renewable energy. However, large deployments of EVs in the foreseeable future will pose major issues in power system operations and electricity markets [1], [2]. Vehicle-to-Grid (V2G) has been proposed as a way of easing potential obstacles in power system operations and increasing the chance for the adoption of EVs [3]. V2G is viewed as a means of exchanging energy and ancillary services between EVs and the electricity grid [4]. A grid-connected EV is capable of providing up/down regulations by adjusting charging rates around the preferred operating point (POP) [5].

A massive penetration of EVs would require a framework pertaining to smart grid applications for optimizing the V2G management [6]. Under this framework, an EV aggregator would be a middleman between an independent system operator (ISO) and individual EVs who offers flexibilities for operating electricity markets. However, EV aggregators encounter uncertainties for V2G management, including the aggregated random behavior of independent customers and the volatility of electricity market prices [7]. Such volatilities which are caused by large penetrations of variable renewable energy resources and random outages of power system components, could pose financial risks to EV aggregators' operations.

The integration of EVs into power grids is an active area of research in which several studies have been published [8]–[11]. The EV aggregators' participation in energy and ancillary services markets was studied in [5], [8], [9] in which various smart charging algorithms were developed. It was demonstrated that smart charging strategies can avoid incremental investments on the power grid infrastructure, reduce network congestion and high energy losses, and prevent renewable energy curtailments. Several sources of uncertainty associated with the EV management were addressed in [10], [11]. The Monte Carlo Simulation (MCS) was used in [10] to evaluate optimal bidding strategies in electricity reserve markets, and uncertain EV management parameters were considered using stochastic programming in [11]. However, EV aggregators' optimal bidding strategies which consider physical and market uncertainties, financial risk management, and bidding options for enhancing the V2G management were not reported in the literature.

In this paper, we propose a stochastic optimization model for optimal bidding strategies of EV aggregators in day-ahead energy and ancillary services markets with variable wind energy. The EV aggregator participates in the ancillary services market by modifying its hourly charging schedule. The forecast errors of EV fleet charging, hourly loads, and wind energy variability, as well as random outages of power generators and transmission lines are considered as potential uncertainties, which are represented in MCS scenarios. The conditional value at risk (CVaR) is utilized as a risk measurement index for managing EV aggregators' financial risks caused by the uncertainties. The EV aggregator's optimal bidding strategy

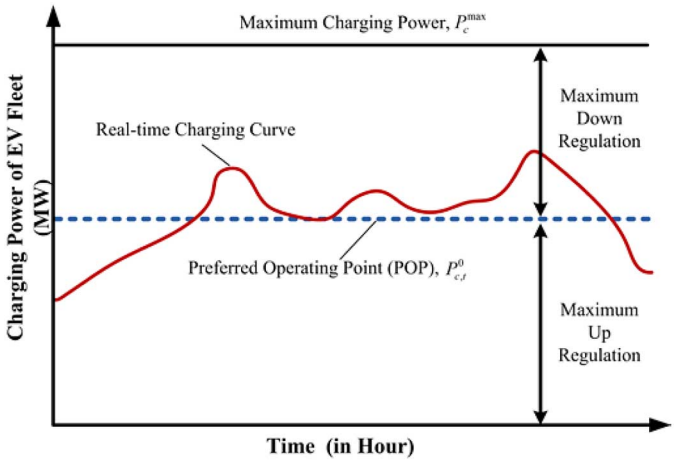

Fig. 1. Provision of up/down regulation service by an EV fleet.

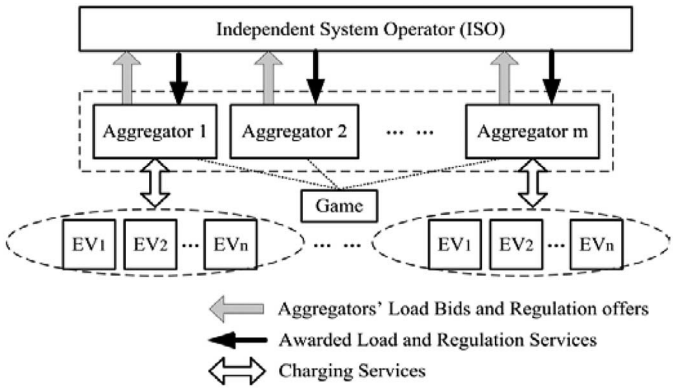

Fig. 2. Day-ahead market framework with EV aggregators.

is formulated as a mathematical programming with equilibrium constraints (MPEC). Accordingly, the aggregators maximize their CVaR in the upper level problem, while the lower level problem minimizes the system operation cost. The bi-level problem is transformed into a single-level mixed integer linear programming (MILP) problem using the primal-dual formulation with linearized constraints. PHA is used to solve the resulting MILP problem. A game theoretic approach is developed for analyzing market competitions among EV aggregators. Numerical cases show the validity of the proposed approach for managing the V2G paradigm.

Here, we develop the-first-of-its-kind EV aggregator bidding model in which MPEC, CVaR, and PHA-based stochastic programming algorithms are considered to address aggregators' optimal bidding strategies. We believe turning the bi-level formulation into MILP and solving it using PHA would result in a slow but effective solution for our complex problem.

The rest of the paper is organized as follows. The features of the proposed model are discussed in Section II. The formulation and solution of the aggregator's optimal bidding strategy is proposed in Section III. The numerical results are presented and analyzed in Section IV. The conclusions are made in Section V.

II. Features of the Proposed Model

A. Regulation Services and EV Characteristics

We assume an EV's interaction with the electricity grid is unidirectional in which the EV would solely draw electric energy from the grid (load only). The characteristics of each EV are aggregated into fleet characteristics as individual EVs do not have an adequate capacity to participate in the energy and ancillary services markets. The EV fleet performs regulation by varying its charging power around its POP as shown in Fig. 1. POP represents the average level of charging power over a specific time period. POP may vary with time and can take any value between zero and its maximum charging power. Fig. 1 illustrates the provision of up/down regulation by the *c-th* EV fleet, where the maximum up/down regulations are dependent on the maximum charging power and the POP. Therefore, the up/down regulations of the EV fleet are performed with only a unidirectional power flow.

In addition to POP, the state of charge (SOC) and energy consumption are the other main parameters for EV fleets. Such parameters are a function of the number of EVs in a fleet. SOC represents the available energy in an EV fleet. The energy consumption in a fleet is dependent on the number of EVs and their energy requirements. The other characteristics in an EV fleet are its travelling patterns, which include starting and destination locations, departure and arrival times at designated locations, and EV charging locations [2]. The travelling pattern determines charging/discharging patterns of EVs in a fleet.

B. Day-Ahead Market Framework With EV Aggregators

EV aggregators act on behalf of individual EVs as individuals cannot directly participate in day-ahead energy markets. The aggregators collect individual EVs' energy information and submit energy bids and regulation offers to the ISO. The ISO aggregates generation and regulation offers as well as demand bids, which are submitted by various market participants including GENCOs, load serving entities (LSE), and EV aggregators. The ISO clears the day-ahead energy and ancillary services markets simultaneously. Fig. 2 shows the day-ahead market framework with EV aggregators. In this paper, we focus on analyzing the impact of individual EV aggregator's bidding strategies in the context of stochastic market operations. A comprehensive market simulation would comprise strategic bidders representing both the generation and the demand sides. This, however, is beyond the scope of this paper and will be investigated in our future work.

C. Monte Carlo Simulation for Representing Uncertainties

The proposed model considers uncertainties in EV fleet characteristics and day-ahead electricity market operations. Random driving behavior of EV drivers could lead to uncertainties in the EV fleet characteristics. Drivers would declare a target level for SOC as individual EVs are connected to the electricity grid. The EV charging is flexible in a manner that the charging requirements would have to be met while aggregators control the battery charging process during flexible charging periods. Moreover, the battery SOC at arrival/ departure times for individual EVs are forecasted, which are based on behaviors

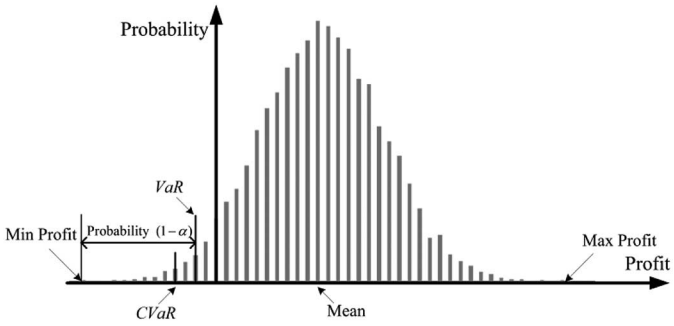

Fig. 3. Illustration of VaR and CVaR.

of drivers, and provided by EV aggregators to the day-ahead market. In this model, forecast errors for daily energy consumptions by EV fleets, arrival/departure times of EVs, and the number of EVs in each fleet are all represented by truncated normal distribution functions, in which the mean values are the forecasts and the standard deviations (STDs) are calculated as percentages of the mean values [2].

The uncertainties in day-ahead market operations include random outages of power system components (generators and transmission lines), and forecast errors for hourly fixed loads and variable wind energy. The fixed load refers to the hourly bus load which has to be satisfied and cannot be curtailed or shifted to other hours. The availability of thermal units and transmission lines are determined based on forced outage rates (FOR) [12]. Hourly load forecast errors are represented by truncated normal distribution functions with a 99.95% confidence interval. The wind speed forecast error is characterized by the auto-regressive moving average (ARMA) with auto correlation factor and diurnal pattern [13].

The MCS method is utilized to generate multiple scenarios for representing uncertainties. In order to improve the MCS efficiency, a low discrepancy method, i.e., Latin Hypercube Sampling (LHS), is used to generate evenly distributed random samples with a smaller variance [12]. A scenario reduction technique with probability metric is used to find a tradeoff between computation speed and accuracy [14].

D. Risk Model for Managing Uncertainties

We use the CVaR for managing EV aggregators' financial risk in uncertain conditions. Fig. 3 illustrates the CVaR of a payoff distribution under α confidence (risk) level, where the value at risk (VaR) is defined as the $(1-\alpha)$ percentile of the payoff distribution; while CVaR is the weighted average payoff in the lower $(1-\alpha)$tail of the payoff distribution (see Fig. 3). If probability distribution functions of random parameters are approximated by inclusion in MCS scenarios, CVaR is calculated by solving the following optimization problem [15]:

$$\underset{\zeta,\delta^s}{\text{Maximize}}\ CVaR = \zeta - \frac{1}{(1-\alpha)}\sum_{s=1}^{NS}\Pr^s\cdot\delta^s$$

subject to

$$\begin{aligned}&\delta^s \geq \zeta - EP^s, s=1,2,\ldots,NS\\ &\delta^s \geq 0, s=1,2,\ldots,NS\end{aligned} \tag{1}$$

where ζ represents VaR (see Fig. 3), EP^s is the scenario s payoff, and δ^s is an auxiliary positive variable representing the difference between VaR and the scenario payoff, if the difference is positive, and is zero if the scenario payoff is greater than VaR.

III. Problem Formulation

The proposed model consists of two submodels which include the aggregators' CVaR maximization model and the market clearing model. These two submodels are discussed below.

A. Aggregator's Payoff

Here, we consider aggregators who buy energy exclusively from a pool-based market. The aggregator's payoff would come from two sources: 1) revenues from selling energy to EV customers minus the cost of buying energy from the pool. The energy purchase through bilateral contracts would be a much simpler case and can be easily included. 2) a fixed share of the revenue that is obtained by providing regulation services. Under this tariff structure, the EV aggregator has an incentive to offer regulation services as much as possible.

We assume that each EV fleet has an aggregated second-order concave demand (energy) payoff function (2) which pays its aggregator at the exact demand payoff.

$$CT_c = -a_c E_c^2 + b_c E_c, \forall c \tag{2}$$

where a_c and b_c are non-negative cost coefficients. The capital investment cost of EV is not considered as part of short-term operation. The *n-th* aggregator's payoff function in scenario s is defined as:

$$\begin{aligned}EP^s =& \sum_{t=1}^{NT}\sum_{c\in\Theta_n}\left[-a_c\cdot\left(E_{c,t}^0\right)^2 + b_c\cdot E_{c,t}^0 - \overline{LMP}_{c,t}^0\cdot E_{c,t}^0\right]\\ &+\beta\cdot\sum_{t=1}^{NT}\sum_{c\in\Theta_n}\left(\bar{\lambda}_{c,t}^{UP}\cdot R_{c,t}^{UP} + \bar{\lambda}_{c,t}^{DN}\cdot R_{c,t}^{DN}\right)\\ &-\sum_{t=1}^{NT}\sum_{c\in\Theta_n}\overline{LMP}_{c,t}^s\cdot\Delta E_{c,t}^s,\ s=1,2,\ldots,NS\end{aligned} \tag{3}$$

where the first line is the payoff for trading energy in the base case and the second line represents the revenue from regulation services. In (3), the first two lines represent the aggregator's revenues collected from the day-ahead energy and ancillary services markets. The third line in (3) denotes the cost of energy deviations in a scenario. The scenario energy deviation represents corrective actions from the base case to a possible realization in the real-time market. One-hour granularity is used in the proposed model, which is consistent with the day-ahead market clearing. The financial settlement is carried out based on the average hourly real-time price, which is practiced in several electricity markets [16].

The objective function of the *n-th* EV aggregator is to determine the base-case hourly charging power, i.e., POP, so that the aggregator's lower-tail weighted average payoff (*CVaR*) is maximized while satisfying EVs' energy requirements and physical constraints.

B. Upper Level: Maximization of Aggregator's CVaR

The EV constraints are listed in (5)–(13). Upward/downward regulation limits are shown in (5) and (6), respectively, where $P^0_{c,t}$ represents the scheduled POP of EV fleet c at time t. Constraint (6) suggests that the downward regulation should be greater than neither the remaining charging power nor the EV battery capacity. Hourly charging energy $E^s_{c,t}$ in each MCS scenario is defined in (7), which is equal to energy purchased in day-ahead and real-time markets, and is restricted by the battery capacity. Limitations on the energy deviation, charging power, and SOC are shown in (8)–(10), respectively. The evolution of SOC over time and charging requirements in the entire flexible charging period are listed in (11) and (12), respectively. Constraint (12) ensures that the charging requirements are satisfied with the energy purchased in day-ahead and real-time markets. The limitation on the aggregator's hourly total charging energy is listed in (13), which may either reflect physical energy limits or be imposed by the ISO. Constraints (14) and (15) incorporate the CVaR metrics.

The aggregator's CVaR maximization model in (4)–(15) integrates the optimal POP selection, also known as the smart charging algorithms [8], [9]. The LMPs and the up/down regulation reserve prices in (3) are provided by the market clearing process. We simulate the market clearing process as follow.

$$\underset{\zeta,\delta^s,P^s_{c,t},E^s_{c,t}}{\text{Maximize}} \; CVaR = \zeta - \frac{1}{(1-\alpha)}\sum_{s=1}^{NS} \Pr^s \cdot \delta^s \tag{4}$$

subject to

$$0 \le R^{UP}_{c,t} \le P^0_{c,t}, c \in \Theta_n, t \in T_c. \tag{5}$$

$$0 \le R^{DN}_{c,t} \le \min\{P^{\max}_c - P^0_{c,t}, SOC^{\max}_c - SOC^0_{c,t}\}, \quad c \in \Theta_n, t \in T_c. \tag{6}$$

$$E^s_{c,t} = E^0_{c,t} + \Delta E^s_{c,t} = P^s_{c,t} \cdot \tau \le SOC^{\max}_c, \quad c \in \Theta_n, t \in T_c, \forall s. \tag{7}$$

$$|\Delta E^s_{c,t}| \le \Delta E^{\max}_c, c \in \Theta_n, t \in T_c, \forall s. \tag{8}$$

$$0 \le P^s_{c,t} \le P^{\max}_c, c \in \Theta_n, t \in T_c, \forall s. \tag{9}$$

$$SOC^{\min}_c \le SOC^s_{c,t} \le SOC^{\max}_c, c \in \Theta_n, t \in T_c, \forall s. \tag{10}$$

$$SOC^s_{c,t+1} = SOC^s_{c,t} + \eta \cdot P^s_{c,t} \cdot \tau, c \in \Theta_n, t \in T_c, \forall s. \tag{11}$$

$$\sum_{t \in T_c} (E^0_{c,t} + \Delta E^s_{c,t}) \ge CREQ_c, c \in \Theta_n, \forall s. \tag{12}$$

$$E^{\min}_{n,t} \le \sum_{c \in \Theta_n} (E^0_{c,t} + \Delta E^s_{c,t}) = PA^s_{n,t} \cdot \tau \le E^{\max}_{n,t}, \forall t, \forall s. \tag{13}$$

$$\delta^s \ge \zeta - \sum_{t=1}^{NT}\sum_{c \in \Theta_n}\left[-a_c \cdot (E^0_{c,t})^2 + b_c \cdot E^0_{c,t} - \overline{LMP}^0_{c,t} \cdot E^0_{c,t}\right] - \beta \cdot \sum_{t=1}^{NT}\sum_{c \in \Theta_n}\left(\bar{\lambda}^{UP}_{c,t} \cdot R^{UP}_{c,t} + \bar{\lambda}^{DN}_{c,t} \cdot R^{DN}_{c,t}\right) + \sum_{t=1}^{NT}\sum_{c \in \Theta_n} \overline{LMP}^s_{c,t} \cdot \Delta E^s_{c,t}, s = 1, 2, \ldots, NS \tag{14}$$

$$\delta^s \ge 0, s = 1, 2, \ldots, NS \tag{15}$$

C. Upper Level: Market Clearing Model

We assume 1) EV aggregator's energy bid is a demand curve where the bidding price drops linearly with the increasing level of demand; 2) EV aggregator's regulation offer is a flat (single segment) curve; 3) GENCOs and LSEs submit offers and bids at their corresponding marginal cost and payoff levels, respectively. The ISO uses a security-constrained economic dispatch (SCED) to clear energy and ancillary services markets simultaneously. The SCED is formulated as a two-stage stochastic linear programing problem, in which the dispatch in the base case is the first-stage decision and the dispatch at the individual scenario level is the second-stage decision. Note that dual variables are provided as subscripts to the corresponding constraints.

The objective function, expressed in (16), is to determine the dispatch for generating resources including wind energy such that the total system operation cost is minimized. The first line in the objective function (16) is the base-case (the first stage) system operation cost including piecewise linear production cost, no-load cost, and piecewise linear startup/shutdown costs. The second line in (16) represents the scenario (the second stage) deviation in thermal generation cost.

The objective function (16) is subject to system and individual component constraints as follows. The system-wide constraints include power balance constraint (17), system up (18) and down (19) regulation reserve requirements, and power flow constraint (20). In (18), the quick-start generators are also capable of offering upward regulation even when they are offline [16]. Constraint (21) shows limits on RES generators. The generating unit operating constraints include energy of thermal units (22) and block generation limit (23), max/min generation limits (24), and inter-temporal ramping up (25) and ramping down (26) limits in the base case.

Dispatch adjustment limits of non-quick-start and quick-start thermal units are shown in (27) and (28), respectively. Such dispatch adjustment is restricted by the thermal unit ramping up/down rate limits [17]. Constraints (27) and (28) guarantee a secure and economic transfer of system operation status from the base case to all scenarios at each time period [17].

Scenario commitments of non-quick start thermal units are the same as those in the base case, which is shown in the third line in (27). However, quick-start units (e.g., natural gas turbines) that are offline in the base case may be committed in any scenario with a transition cost of $FT^s_{i,t}$ expressed in (29).

Constraint (29) shows that the transition cost of quick-start units comprises corrective dispatch costs and startup costs from the base case to the scenario. Here, unit commitment states $\bar{I}^0_{i,t}$ and $\bar{I}^s_{i,t}$ are assumed to be known *a priori* in the market clearing problem. The LMPs are calculated by using dual variables φ^s_t in (17) and $\tilde{\pi}, \underset{\sim}{\pi}$ in (20); the up/down regulation reserve prices are obtained based on dual variables $\lambda^{UP}_t, \lambda^{DN}_t$ in (18)–(19).

$$\min \left\{ \sum_{t=1}^{NT} \sum_{i \in Q \cup NQ} \left[\sum_{m=1}^{NM} \mu_{m,i,t} \cdot PG^0_{m,i,t} + NL_i \cdot \bar{I}^0_{i,t} + \overline{SU}^0_{i,t} + \overline{SD}^0_{i,t} \right] \right\} + \sum_{s=1}^{NS} \Pr^s \cdot \sum_{t=1}^{NT} \left[\sum_{i \in NQ} \sum_{m=1}^{NM} \mu_{m,i,t} \cdot \Delta PG^s_{m,i,t} + \sum_{i \in Q} FT^s_{i,t} \right] \tag{16}$$

subject to:

$$\sum_{i=1}^{NG} PG^s_{i,t} + \sum_{k=1}^{NK} PR^s_{k,t} = \sum_{n=1}^{NA} \overline{PA}^s_{n,t} + \sum_{d=1}^{NB} PD^s_{d,t} : \varphi^s_t, \forall t, \forall s. \tag{17}$$

$$\sum_{n=1}^{NA} \sum_{c \in \Theta_n} R^{UP}_{c,t} + \sum_{i=1}^{NG} RG^{UP}_{i,t} + \sum_{i \in Q} QSC_i \geq REQ^{UP}_t : \lambda^{UP}_t, \forall t \tag{18}$$

$$\sum_{n=1}^{NA} \sum_{c \in \Theta_n} R^{DN}_{c,t} + \sum_{i=1}^{NG} RG^{DN}_{i,t} \geq REQ^{DN}_t : \lambda^{DN}_t, \forall t \tag{19}$$

$$-\mathbf{PL^{max}} \leq \mathbf{SF} \times [\mathbf{K_P} \times \mathbf{P^s} - \mathbf{K_D} \times (\overline{\mathbf{PA}}^{\mathbf{s}} + \mathbf{PD^s})] \leq \mathbf{PL^{max}} : \tilde{\boldsymbol{\pi}}, \underset{\sim}{\boldsymbol{\pi}} \tag{20}$$

$$0 \leq PR^s_{k,t} \leq G^{f,s}_{k,t}, \forall k, \forall t, \forall s. \tag{21}$$

$$PG^s_{i,t} = \sum_{m=1}^{NM} PG^s_{m,i,t}, \forall i, \forall t, \forall s. \tag{22}$$

$$0 \leq PG^s_{m,i,t} \leq PG^{\max}_{m,i,t}, \forall m, \forall i, \forall t, \forall s. \tag{23}$$

$$PG^{\min}_i \cdot \bar{I}^s_{i,t} \leq PG^s_{i,t} \leq PG^{\max}_i \cdot \bar{I}^s_{i,t}, \forall i, \forall t, \forall s. \tag{24}$$

$$PG^0_{i,t} - PG^0_{i,t-1} \leq RU^{\max}_i + M \cdot (2 - \bar{I}^0_{i,t-1} - \bar{I}^0_{i,t}), \forall i, \forall t. \tag{25}$$

$$PG^0_{i,t-1} - PG^0_{i,t} \leq RD^{\max}_i + M \cdot (2 - \bar{I}^0_{i,t-1} - \bar{I}^0_{i,t}), \forall i, \forall t. \tag{26}$$

$$\begin{aligned} &PG^s_{i,t} - PG^0_{i,t} \leq RU^{\max}_i \cdot \bar{I}^s_{i,t}, \\ &PG^0_{i,t} - PG^s_{i,t} \leq RD^{\max}_i \cdot \bar{I}^s_{i,t}, \\ &\bar{I}^0_{i,t} = \bar{I}^s_{i,t}, \quad i \in NQ, \forall t, s = 1, 2, \ldots, NS. \end{aligned} \tag{27}$$

$$\begin{aligned} &PG^s_{i,t} - PG^0_{i,t} \leq (RU^{\max}_i - QSC_i) \cdot \bar{I}^0_{i,t} + QSC_i, \\ &PG^0_{i,t} - PG^s_{i,t} \leq (RD^{\max}_i - PG^{\max}_i) \cdot \bar{I}^0_{i,t} + PG^{\max}_i, \\ &\qquad i \in Q, \forall t, s = 1, 2, \ldots, NS. \end{aligned} \tag{28}$$

$$FT^s_{i,t} = \sum_{m=1}^{NM} \mu_{m,i,t} \cdot \Delta PG^s_{m,i,t} + \overline{SU}^s_{i,t} \cdot \max(0, \bar{I}^s_{i,t} - \bar{I}^0_{i,t}), \quad i \in Q, \forall t, \forall s \tag{29}$$

D. Conversion of the Bi-level Model into a Single-Level Stochastic Model

The aggregator's optimal bidding strategy is modeled in (4)–(29) as a bi-level nonlinear LP (NLP) problem where the upper level problem corresponds to the aggregators' CVaR maximization and the lower level problem corresponds to the simulated market clearing process, i.e., minimization of the system production cost. There are two categories of non-linearities associated with constraint (14):

a) The aggregator's payoff function (3) is maximized in terms of the lower-tail weighted average. The quadratic terms, i.e., $-a_c \cdot (E^0_{c,t})^2 + b_c \cdot E^0_{c,t}$ shown on the first line of (14), are continuous and twice differentiable with negative-definite Hessian matrix. Thus, the quadratic terms are strictly concave in a maximization problem. In such a case, the piecewise linear approximation can be simply transformed into a linear programming [18]. This is similar to the case dealing with the convex fuel cost for thermal units in SCED [19].
b) The other category of non-linearity lies in the multiplication of two continuous variables, such as $\overline{LMP}^0_{c,t} \cdot E^0_{c,t}$, $\bar{\lambda}^{UP}_{c,t} \cdot R^{UP}_{c,t}$, $\bar{\lambda}^{DN}_{c,t} \cdot R^{DN}_{c,t}$, and $\overline{LMP}^s_{c,t} \cdot \Delta E^s_{c,t}$ in (14), which are derived respectively from lower- and upper-level problems. They can be approximated as a MILP formulation by dividing the continuous variables into multiple triangles with affine function [20].

By linearizing the nonlinear terms in (14), the bi-level NLP problem (4)–(29) is transformed into an equivalent single-level stochastic MILP problem. The problem is procured by maximizing (4) in the upper-level problem, while taking into account constraints (5)–(15) of each upper-level problem, the primal and dual forms of constraints (17)–(29) of the lower-level market clearing problem, and the strong duality theorem (SDT) equation of the lower level problem.

To overcome the computational complexity of the stochastic optimization, we further employ PHA to solve the resulting stochastic MILP. The PHA is a scenario-based decomposition technique which has been utilized as an efficient way to solve various types of stochastic problems [21]–[23]. The PHA will first relax non-anticipativity constraints, i.e., base-case continuous variables should be equal across all scenarios, and then solve each scenario independently. A mechanism for increasing penalty factors will then be introduced to penalize scenario deviations from the corresponding implementable solution. It is guaranteed that the non-anticipativity constraints will be satisfied once the PHA converges.

E. EV Aggregators' Game

Suppose there are *NA* aggregators. We use the supply function equilibrium (SFE) to model the n-th $(n = 1, 2, \ldots, NA)$ aggregator's strategic bidding. SFE enables an aggregator to

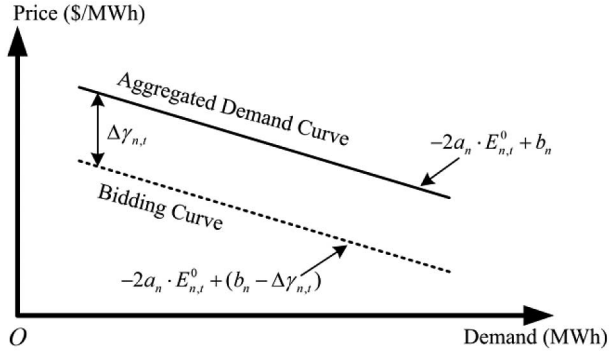

Fig. 4. Demand and bidding curves of the *n-th* EV aggregator.

link its bidding price with the bidding quantity of its energy demand. Fig. 4 shows the bidding curve of an aggregator in the day-ahead market. Here, the aggregator controls the charging of EV fleet and manipulates the $(b_n - \Delta\gamma_{n,t})$ intercept of the bid curve rather than its slope a_n. The reason for this assumption is that, according to our experience, a unique solution would rarely exist if both a_n and b_n are manipulated. In this case, the unique equilibrium would only exist under very restrictive conditions [24].

In a complete information game, the *n-th* EV aggregator will not only have the knowledge of its own payoff function (3), but also knows its opponents' payoff functions. However, this is not usually the case in a competitive electricity market, where each EV aggregator would know its own payoffs function, but may lack such information of other aggregators. Therefore, each EV aggregator would model its opponents into different types. Here, an EV aggregator's type corresponds to the biding curve specified by coefficients a_n and b_n.

Suppose the *n*-th EV aggregator has $|TP_n|$ types. Let $\mathbf{TP}_n$ be the type space of the *n*-th aggregator with tp_n as an element, and $\mathbf{TP}_{-n} = \mathbf{TP}_1 \times \mathbf{TP}_2 \times \ldots \mathbf{TP}_{n-1} \times \mathbf{TP}_{n+1} \times \ldots \times \mathbf{TP}_{NA}$ denote the types of the *n*-th aggregator's opponents with $\mathbf{tp}_{-n}$ as an element. Let $\Pr(\mathbf{tp}_{-n}|tp_n)$ be the conditional probability when the *n*-th aggregator is type $tp_n$and its opponents' type is $\mathbf{tp}_{-n}$. $\mathbf{\Delta\gamma_n}(tp_n)$is the bidding strategy vector for the *n*-th aggregator when its type is tp_n, while $\mathbf{\Delta\gamma_{-n}}(\mathbf{tp}_{-n})$is the bidding strategy vector of the *n*-th Aggregator's opponents when their types are represented by $\mathbf{tp}_{-n}$. Based on the Harsanyi transformation [25], the payoff function of aggregator n at scenario s is equivalent to its expected revenue for type pairs $(tp_n, \mathbf{tp}_{-n})$ as:

$$\sum_{tp_n \in \mathbf{TP}_n} \sum_{\mathbf{tp}_{-n} \in \mathbf{TP}_{-n}} EP_n^s(tp_n, \mathbf{\Delta\gamma_n}(tp_n), \mathbf{\Delta\gamma_n}(\mathbf{tp}_{-n})) \cdot \Pr(\mathbf{tp}_{-n}|tp_n) \cdot \Pr(tp_n) \quad (30)$$

In (30), the incomplete game is transformed to a complete game with imperfect information by using the corresponding joint probability distribution of the game [24], [25].

The sensitivity of the *n-th* aggregator's payoff to its energy bidding strategy is given in (31), where the sub/upper scripts are neglected for simplicity.

$$\frac{\partial EP}{\partial \Delta\gamma} = \frac{\partial EP}{\partial E} \cdot \frac{\partial E}{\partial \Delta\gamma} + \frac{\partial EP}{\partial LMP} \cdot \frac{\partial LMP}{\partial \Delta\gamma} \quad (31)$$

and $\partial EP/\partial E$ and $\partial EP/\partial LMP$ are calculated according to (3). However, in practice, $\partial E/\partial\Delta\gamma$ and $\partial LMP/\partial\Delta\gamma$, which represent sensitivities of the awarded energy and the LMP to bidding strategies, may not be calculated easily. The bidding strategy will impact the awarded energy at the upper level and the LMP at the lower level. The upper-level awarded energy is one part of the corresponding bus load at the lower level, as shown in (17). However, the exact relations among those variables are difficult to obtain analytically. Instead, they are normally modeled by simulation, regression, game theory, and heuristics [25]. Here, a linear regression method is adopted to approximate the relations between the bidding strategy and the awarded energy and that of the LMP, based on historical data, which are shown as follows:

$$E = \varphi_1 \cdot \Delta\gamma + \varphi_2 \quad (32)$$

$$LMP = \phi_1 \cdot \Delta\gamma + \phi_2 \quad (33)$$

The EV aggregator would update its bidding strategy according to (34) until its payoff is maximized.

$$\Delta\gamma^{j+1} = \Delta\gamma^j + \frac{\partial EP}{\partial \Delta\gamma^j} \cdot \nu \quad (34)$$

where j is the index for iterations and ν is a step size. Similar procedures can be developed for updating regulation services offers, where the difference is that a flat (single segment) regulation offer is considered and the marginal cost of regulation service is assumed to be zero in this model. Theoretically, the Nash equilibrium would be found when no EV aggregator has any incentives to unilaterally change its bids and offers.

We adopt the following steps, shown in Fig. 5, for calculating the EV aggregator's Nash equilibrium:

Step 1): The *n*-th EV aggregator estimates other aggregators' types and their joint probability distribution based on the published market information. Set the initial values $\Delta\gamma_{n,t}, \lambda^{UP}_{n,t}, \lambda^{DN}_{n,t}$ for aggregators.

Step 2): Suppose opponents' bidding strategies are fixed and use (32) to set the opponents' initial awarded energy. Solve the bi-level model for the *n-th* aggregator and update its bidding strategy using (34) until no EV aggregator would change its bidding strategy.

Step 3): Repeat Step 2) to find the aggregator's optimal bidding strategies in response to its opponents' bidding strategies.

Step 4): Repeat Steps 2) and 3) until no aggregator would change its bidding strategy.

It is guaranteed that the above steps will find one equilibrium point as long as a Nash equilibrium exists. When multiple Nash equilibria exist, the proposed steps may find the global Nash equilibrium if a good initial bidding strategy is given. In such cases, EV aggregators' historical bids and offers can be used as initial bidding strategies.

IV. Numerical Results

In this section, a modified 6-bus power system and a modified IEEE 118-bus system are applied to study the proposed approach, which is implemented in Microsoft Visual C++ on an Intel Xeon Sever with 64 GB RAM. The proposed problem

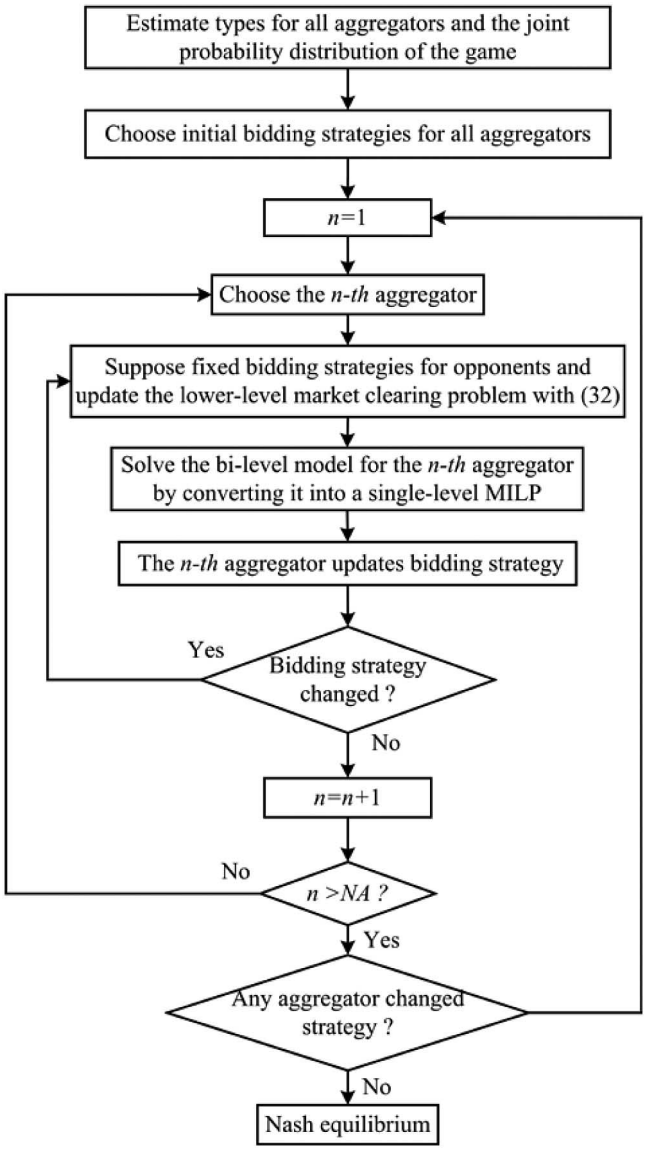

Fig. 5. EV Aggregation Solution for Calculating the Nash equilibrium.

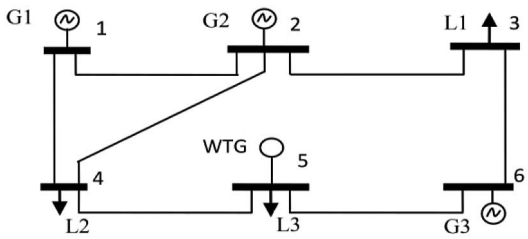

Fig. 6. One line diagram of 6-bus system.

for each aggregator is solved by using ILOG CPLEX 11.0 [26]. The scenario reduction is executed by applying SCENRED in the General Algebraic Modeling System (GAMS).

A. The Modified 6-Bus System

The 6-bus system, shown in Fig. 6, has one wind energy system, seven transmission lines, and three thermal units. The thermal generating units, transmission lines and the expected hourly inflexible load data are given in [19]. The wind energy capacity is 40 MW. The forecasted wind speed time series is obtained by implementing the Markov process transition probability matrix (TPM), which is characterized by the probability distribution parameters of wind speed time series [27]. The system inflexible peak demand is 256 MW at Hour 17. The daily RES generation forecast is 478 MWh and the total system demand is 4,985 MWh. Therefore, the penetration of the available wind generation is 9.6% in the case study. The STD of hourly inflexible load is 5%. FORs of thermal units and transmission lines are 2% and 1%, respectively.

There are three EV aggregators in Bus 5, each owning an EV fleet. A normal charging mode (level 2) is considered with a maximum charging power of 12 kW for each individual EV. The battery capacity, initial SOC, maximum charging power and coefficients of marginal payoff for EVs are aggregated into fleet characteristics in Table I. The charging efficiency of the EV is 90% ($\eta = 0.9$). Table II shows five traveling patterns for EVs and their expected daily energy consumption. Percentages of EVs in a fleet that are categorized into different travel patterns are shown in Table III. The forecast errors of daily energy consumption, arrival/departure time, and the number of EVs in a fleet are represented by truncated normal distribution functions, with their mean, STD, max, and min values listed in Table IV. The confidence (risk) level is 95% ($\alpha = 0.95$) and the share of revenue from the regulation service is 50% ($\beta = 0.5$). 1,800 scenarios are originally generated by MCS, which are reduced to 185 by the scenario reduction technique based on probability metrics.

TABLE I
AGGREGATED CHARACTERISTICS FOR EV AGGREGATORS

Aggr. Index	EV fleet Index	No. of EVs	Battery Capacity. (MWh)	Initial SOC (%)	Max Charge (MW)	a ($/MWh^2)	b ($/MWh)
1	1	1500	65.76	15	18.00	0.21	60
2	2	1300	56.94	15	15.60	0.25	55
3	3	1000	42.73	15	12.00	0.27	50

TABLE II
TRAVEL PATTERNS FOR INDIVIDUAL EVS

Pattern No.	Arrival		Departure		Exp. Daily Energy Consumption (kWh)
	Time	Bus	Time	Bus	
1	20:00	5	6:30	1	26.50
2	19:30	5	7:00	2	23.70
3	20:30	5	6:00	3	28.50
4	19:30	5	7:15	4	20.40
5	19:15	5	7:30	6	19.50

TABLE III
PERCENTAGE OF EVS IN EACH TRAVEL PATTERN

Pattern No.	Aggregator #1 (%)	Aggregator #2 (%)	Aggregator #3 (%)
1	25	20	10
2	20	10	15
3	30	25	10
4	15	25	30
5	10	20	35

TABLE IV
TRUNCATED NORMAL DISTRIBUTIONS FOR EV UNCERTAINTIES (NORMALIZED)

	Mean	STD	Max	Min
Daily energy consumption	1	0.10	1.35	0.65
Arrival and departure time	1	0.05	1.18	0.83
Number of EVs in a fleet	1	0.02	1.07	0.93

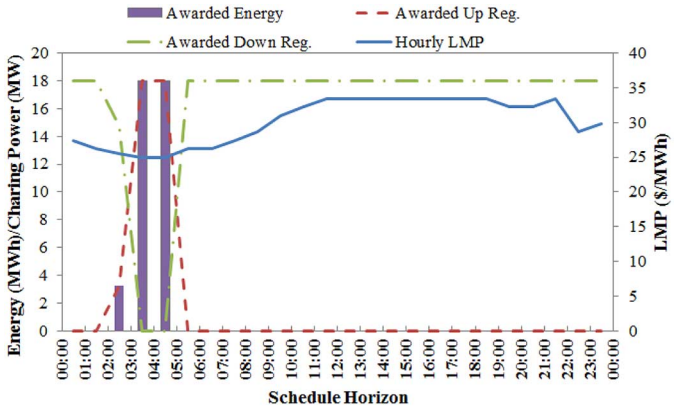

Fig. 7. Awarded hourly energy bids and up/down regulation offers.

Four cases are studied to illustrate the impact of the EV aggregator's bidding strategy on power market operations:

Case 1: Consider Aggregator 1 is the only EV aggregator that participates in the market.

Case 2: Compare the impact of different charging modes on the day-ahead scheduling.

Case 3: Consider the impact of risk levels on the aggregator's payoff.

Case 4: Consider the effect of gaming on Aggregators 1-3.

These cases are discussed as follows:

Case 1: Aggregator 1 is the only market participant considered in this case, where $\Delta\gamma_{n,t}$ is 15 \$/MWh and $\lambda^{UP}_{n,t}$, $\lambda^{DN}_{n,t}$ are priced at 2.5 \$/MW. The commitment states of thermal units are known as *ex ante*, where Unit 2 is not committed in the scheduling horizon; while Unit 1 is always committed and Unit 3 is only committed at peak hours. The awarded hourly energy bids and up/down regulation offers are illustrated in Fig. 7. The energy bids are awarded from 2:00 to 5:00 and hourly charging power reaches the maximum of 18 MW from 03:00 to 5:00. The upward regulation offers are awarded at the same hours since the upward regulation is less than or equal to awarded energy according to (5). In addition, the downward regulation reaches the maximum charging power from 0:00 to 2:00, and 5:00 to the midnight of the second day.

Here, the maximum up/down regulations are awarded for managing the variability of wind energy. The aggregator's payoff is listed in Table V. An expected payoff of \$1,741 and payoff STD of \$305 are obtained, in which $641/1741 = 36.8\%$ of the total payoff is derived from the energy price markup, while $1100/1741 = 63.2\%$ of the total payoff is from selling regulation services. The results in Table V verify that a large proportion of aggregator's payoff may come from regulation services [9] which further necessitates the inclusion of regulation services in the aggregator's bidding portfolio.

TABLE V
PAYOFF COMPONENTS OF THE AGGREGATOR

Expected Payoff ($)	STD of Payoff ($)	Energy Payoff ($)	Reg. Services Payoff ($)
1,741	305	641	1,100

TABLE VI
COMPARISON OF DIFFERENT CHARGING MODES

	Proposed Charging	Central Dispatch	Inflexible Charging
Average Load Cost ($/MWh)	31.6	31.2	37.1
Average LMP ($/MWh)	32.8	32.6	33.7
System Operation Cost ($)	689,541	687,655	728,014

Case 2: As discussed in Section III.A, the proposed optimal bidding strategy includes the smart charging algorithm. Thus, the results obtained using three different charging algorithms are compared in this case, in which the proposed charging algorithm is contrasted with central dispatch and inflexible charging methodologies. The central dispatch is the hourly charging scheduled by an ISO, where the total social welfare of generation supplier and consumer is maximized while satisfying constraints (5)–(13) and (17)–(29). The inflexible charging demand is uncontrolled demand (charging) in a sense that each EV driver would start to charge the vehicle as soon as it is parked. The uncontrollable charging will stop when the EV's stated energy requirement is reached.

The average load cost (\$/MWh), average LMP, and system operation cost in the three different charging models are shown in Table VI, where the average load cost is calculated by dividing the total load payment by the total load. As expected, the central dispatch is the most efficient charging mode. However, this mode is unrealistic since the ISO cannot directly control the charging process of each EV fleet. In Table VI, the differences between the proposed charging and central dispatch are shown to be small, which imply that the proposed smart charging algorithm will not significantly affect the efficiency of the day-ahead market, if the aggregators do not exercise market power. In contrast, the inflexible charging leads to a higher average load cost, average LMP, and system operation cost, in which a substantial increase, $(37.1 - 31.2)/31.2 = 18.9\%$ in the average load cost is attributed to the EV charging at peak load hours. This result demonstrates the effectiveness of the proposed smart charging algorithm, which is embedded in the aggregator's MPEC model.

Case 3: In this case, the proposed problem is solved for different risk levels. The impact of risk level on the Aggregator 1's payoff is shown in Table VII.

When $\alpha = 0.0$, the Aggregator will not be concerned with the risk level (i.e., risk seeking), and will maximize its expected payoff, which leads to the highest expected payoff \$2,023 and highest standard deviation \$488. As the risk level is increased, the Aggregator tends to take a lower risk option which will result in a lower expected payoff and STD of payoff. When $\alpha = 0.99$, the Aggregator is not willing to take any risks (i.e., risk-averse case), which will result in the lowest expected payoff \$1,647 and the lowest STD of payoff \$277. Comparing

TABLE VII
EXPECTED PAYOFF AND STD VERSUS CONFIDENCE LEVEL

α	Expected Payoff ($)	STD of Payoff ($)
0.00	2023	488
0.10	1998	451
0.30	1946	413
0.50	1896	399
0.70	1801	356
0.99	1647	277

TABLE VIII
NASH EQUILIBRIUM IN A 3-AGGREGATOR GAME FOR 6-BUS SYSTEM

	A1	A2	A3
Awarded Energy Bids (MWh)	41.2	36.0	24.4
Awarded Reg. Offers (MW)	454	372	253
Daily Payoff ($)	1682±273	1121±172	501±74
Number of Iterations=164		CPU Time=4728 sec	

risk-seeking and risk-averse cases, the Aggregator's expected payoff is decreased by $(2,023-1,647)/2,023=18.6\%$ and the STD of payoff by $(488-277)/488=43.2\%$. The results in Table VI suggest that the risk level taken by the Aggregator has a significant impact on its expected and the STD of payoff. The Aggregator could effectively manage its risk by identifying an appropriate risk level for itself.

Case 4: Competition among Aggregators 1–3 (i.e., three-player game) is considered in this case. We assume each aggregator's type is known to other market participants based on the historic data shown in Tables I–IV. Table VIII shows the results of the game theoretic approach where the initial bidding strategies are chosen randomly within their corresponding lower and upper bounds. In Table VIII, "±" indicates the 95% confidence interval for an uncertainty.

In this case, each aggregator's energy demand is satisfied during its flexible charging period. Moreover, Aggregator 1 has the largest energy and regulation reserve awards since it has the largest number of EVs in its fleet. In Table VIII, Aggregator 1 possesses the largest daily payoff of all 3 aggregators and the difference between the daily payoffs of Aggregators 1 and 3 is significant, i.e., $(1682-501)/1682=70.2\%$. This is because Aggregator 1 has a higher payoff margin when its aggregated marginal payoff (see Table I) is higher than that of Aggregator 3. In addition, the Aggregator 3's energy requirement is satisfied at higher LMPs (off-valley hours) due to the power network constraints. The results in Table VIII suggest that an aggregator that owns a larger number of EVs in its fleet will have a larger market power, which can make the EV aggregator more profitable in energy and regulation markets. A Nash equilibrium is obtained after 164 iterations with 4,728 seconds of CPU time in such a small-scale system.

B. The Modified 118-Bus System

Case studies in a larger-scale system are performed primarily to show the scalability of the proposed solution method. The modified IEEE-118 bus system has 54 thermal units, 186 branches, and 91 load buses. The parameters of generators, transmission network, and load profiles are given in [19]. There are 3 geographically dispersed wind farms located at Buses 15, 54 and 96, respectively. The daily wind generation forecast is 22,845 MWh and the total system load is 113,506 MWh. Therefore, the wind penetration level is 20.1% in this system. FORs of thermal units and transmission lines are the same as in the modified 6-bus system. We also adopt three EV aggregators located at Bus 96, each managing an EV fleet.

TABLE IX
NASH EQUILIBRIUM IN A 3-AGGREGATOR GAME FOR 118-BUS SYSTEM

	A1	A2	A3
Awarded Energy Bids (MWh)	41.5	36.1	24.5
Awarded Reg. Offers (MW)	458	379	261
Daily Payoff ($)	3321±345	1859±222	998±173
Number of Iterations=148		CPU Time=9044 sec	

The travel patterns of EVs are the same as those listed in Table II with the following differences: 1) the arrival bus is Bus 95 for all patterns; and 2) the departure buses for Patterns 1–5 are Buses 82, 83, 93, 94, and 96, respectively. Other parameters associated with each EV fleet are the same as those stated in the modified 6-bus system. We initially generate 625 MCS scenarios and then reduce the number to 80 by the fast backward/forward method in SCENRED.

Table IX shows the Nash equilibrium in which each EV's energy demand is met by the departure time. Note that since the parameters of EV aggregators are the same as those in the 6-bus system, the awarded energy bids and regulation offers for each aggregator are very close to those in Table VIII. In addition, Aggregator 1 has the dominant energy and regulation reserve awards which offer the largest daily payoff of all 3 aggregators. However, as opposed to the 6-bus system, the LMP at Bus 95 is much lower than that at Bus 5, leading to a significantly higher daily payoff for each aggregator. A Nash equilibrium is procured in this system after 148 iterations with 9,044 seconds of CPU time. The iteration number is smaller than that of the 6-bus system, which shows the scalability of the proposed approach for finding a Nash equilibrium; However, the overall CPU time is nearly doubled as the size of lower-level market clearing problem is increased significantly.

The 2.5-hour solution time for the stochastic case can further be reduced in practice by considering the specific characteristics of power systems, heuristic assumptions for power system operations, and the introduction of parallel processing. In essence, the computation efficiency can further be improved by 1) providing good estimates of initial bidding strategies so as to reduce the number of iterations; 2) applying either parallel computing techniques or ordinal optimization [28]. The use of PHA allows for the implementation of parallel computing framework, where the MIP solver would solve all scenarios corresponding to much simpler MILP problems simultaneously.

V. CONCLUSIONS

The increased penetration of EVs offers unique economic and environmental opportunities and introduces new challenges in electricity market operations. The EV aggregator would be

an entity that has a function similar to that of a distribution system operator and will participate in the bulk power market operation by submitting bidding strategies. Such distributions system entities, which will perform demand response and manage distributed resources, are gaining widespread attentions in power system operations. This paper proposes a stochastic optimization model for optimal bidding strategies of EV aggregator in day-ahead energy and ancillary services markets with the integration of variable wind energy. Numerical results on the modified 6-bus system and the 118-bus system indicate the effectiveness of the proposed approach for analyzing an aggregator's optimal bidding strategy. The results also show that a large percentage of an aggregator's payoff could stem out of regulation services, and the aggregator could effectively manage its risk by using CVaR. The proposed model can be used by EV aggregators for performing risk-payoff analyses in stochastic market operations.

The application of PHA allows us to investigate a much larger number of scenarios in the stochastic optimization. As a result, we investigated 185 reduced scenarios out of 1800 for the 6-bus system and 80 reduced scenarios out of 625 for the 118-bus system. The increase in simulated scenarios significantly increases the accuracy of the scenario reduction method in terms of ζ_1 relative distance [14]. It is proven that a reduction of the scenario tree by 90% of the original scenarios could still carry almost 75% of relative accuracy [14]. Policies comparison in post-analysis may be another way of evaluating two uncertainty sets. This, however, is out of the scope of this paper and will be addresses in our subsequent work. We will also simulate multiple categories of strategic bidders in our future studies from both the generation and the demand side viewpoint [19], [24].

ACKNOWLEDGMENT

The authors would like to thank the technical support provided by the Science and Technology Unit, King Abdulaziz University, Jeddah, Saudi Arabia.

REFERENCES

[1] J. A. P. Lopes, F. J. Soares, and P. M. R. Almeida, "Integration of electric vehicles in the electric power system," *Proc. IEEE*, vol. 99, no. 1, pp. 168–182, Jan. 2011.

[2] M. E. Khodayar, L. Wu, and M. Shahidehpour, "Hourly coordination of electric vehicle operation and volatile wind power generation in SCUC," *IEEE Trans. Smart Grid*, vol. 3, no. 3, pp. 1271–1279, Sep. 2012.

[3] W. Kempton and J. Tomic, "Vehicle-to-grid power implementation: From stabilizing the grid to supporting large-scale renewable energy," *J. Power Sources*, vol. 144, no. 1, pp. 280–294, Jun. 1, 2005.

[4] W. Kempton and J. Tomic, "Vehicle-to-grid power fundamentals: Calculating capacity and net revenue," *J. Power Sources*, vol. 144, no. 1, pp. 268–279, Jun. 1, 2005.

[5] E. Sortomme and M. A. El-Sharkawi, "Optimal charging strategies for unidirectional vehicle-to-grid," *IEEE Trans. Smart Grid*, vol. 2, no. 1, pp. 131–138, Mar. 2011.

[6] K. Clement-Nyns, E. Haesen, and J. Driesen, "The impact of charging plug-in hybrid electric vehicles on a residential distribution grid," *IEEE Trans. Power Syst.*, vol. 25, no. 1, pp. 371–380, Feb. 2010.

[7] M. Shahidehpour, "Electric vehicles in volatile power system operations," in *Proc. IEEE Power Energy Soc. Gen. Meeting*, Detroit, MI, USA, Jul. 2011.

[8] N. Rotering and M. Ilic, "Optimal charge control of plug-in hybrid electric vehicle in deregulated electricity markets," *IEEE Trans. Power Syst.*, vol. 26, no. 3, pp. 1021–1029, Aug. 2011.

[9] S. I. Vagropoulos and A. G. Bakirtzis, "Optimal bidding strategy for electric vehicle aggregators in electricity markets," *IEEE Trans. Power Syst.*, vol. 28, no. 4, pp. 4031–4041, Nov. 2013.

[10] C. Sandels, U. Franke, N. Ingvar, L. Nordstrom, and R. Hamren, "Vehicle to grid—Monte Carlo simulations for optimal aggregator strategies," in *Proc. Int. Conf. Power System Technol.*, Hangzhou, China, Oct. 2010, pp. 1–8.

[11] M. Shafie-Khah *et al.*, "Modeling of interactions between market regulations and behavior of plug-in electric vehicle aggregators in a virtual power market environment," *Energy*, vol. 40, no. 1, pp. 139–150, Apr. 2012.

[12] L. Wu, M. Shahidehpour, and T. Li, "Stochastic security-constrained unit commitment," *IEEE Trans. Power Syst.*, vol. 22, no. 2, pp. 800–811, May 2007.

[13] A. Boone, "Simulation of short-term wind speed forecast errors using a multi-variate ARMA (1,1) time-series model," M.S. thesis, KTH Royal Inst. of Technol., Stockholm, Sweden, 2005.

[14] J. Dupacová, N. Gröwe-Kuska, and W. Römisch, "Scenario reduction in stochastic programming: An approach using probability metrics," *Math. Program.*, vol. A 95, pp. 493–511, 2003.

[15] R. T. Rockefeller and S. Uryasev, "Conditional value-at risk for general loss distributions," *J. Bank. Finance*, vol. 26, no. 7, pp. 1443–1471, 2002.

[16] PJM, *PJM Manual 11: Energy & Ancillary Services Market Operations* [Online]. Available: http://www.pjm.com/~/media/documents/manuals/~August 2015

[17] L. Wu, M. Shahidehpour, and T. Li, "Comparison of scenario-based and interval optimization approaches to stochastic SCUC," *IEEE Trans. Power Syst.*, vol. 27, no. 2, pp. 913–921, May 2012.

[18] R. J. Vanderbei, *Linear Programming: Foundations and Extensions*. Norwell, MA, USA: Kluwer, 1996.

[19] M. Shahidehpour, H. Yamin, and Z. Li, *Market Operations in Electric Power Systems*. Hoboken, NJ, USA: Wiley, 2002.

[20] S. Kamalinia, L. Wu, and M. Shahidehpour, "Stochastic midterm coordination of hydro and natural gas flexibilities for wind energy integration," *IEEE Trans. Sustain. Energy*, vol. 5, no. 4, pp. 1070–1079, Oct. 2014.

[21] J.-P. Watson and D. L. Woodruff, "Progressive hedging innovations for a class of stochastic mixed-integer resource allocation problems," *Comput. Manag. Sci.*, vol. 8, pp. 355–370, Nov. 2011.

[22] S. Ryan, R. Wets, D. Woodruff, C. Silva-Monroy, and J. Watson, "Toward scalable, parallel progressive hedging for stochastic unit commitment," in *Proc. IEEE Power Eng. Soc. Gen. Meeting*, Jul. 2013, pp. 1–5.

[23] H. Wu *et al.*, "An assessment of the impact of stochastic day-ahead SCUC on economic and reliability metrics at multiple timescales," in *Proc. IEEE Power Eng. Soc. Gen. Meeting*, Jul. 2015, pp. 1–5.

[24] T. Li and M. Shahidehpour, "Strategic bidding of transmission-constrained GENCOs with incomplete information," *IEEE Trans. Power Syst.*, vol. 20, no. 1, pp. 437–447, Feb. 2005.

[25] J. Harsanyi, "Games with incomplete information played by 'Bayesian' players," *Management Science*, vol. 14, no. 3, pp. 159–192, Nov. 1967.

[26] ILOG CPLEX. (2011). *ILOG CPLEX Homepage* [Online]. Available: http://www.ilog.com

[27] J. F. Manwell *et al.*, *Hybrid2-a Hybrid System Simulation Model Theory Manual*. Renewable Energy Research Laboratory, Department of Mechanical Engineering, University of Massachusetts, Amherst, MA, USA, Jun. 2006.

[28] H. Wu and M. Shahidehpour, "Stochastic SCUC solution with variable wind energy using constrained ordinal optimization," *IEEE Trans. Sustain. Energy*, vol. 5, no. 2, pp. 379–388, Apr. 2014.

Hongyu Wu (M'09) received the B.S. degree in energy and power engineering and the Ph.D. degree in the system engineering both from Xi'an Jiaotong University, Xi'an, China, in 2003 and 2011, respectively. He is a Research Engineer at the Power Systems Engineering Center, the National Renewable Energy Laboratory (NREL), Golden, CO, USA. Prior to joining NREL, he was a Visiting Scientist at the Robert W. Galvin Center for Electricity Initiative, Illinois Institute of Technology, Chicago, IL, USA. His research interests include stochastic optimization of large-scale systems, distributed renewable energy integration in smart grid, and home/building energy management systems.

Mohammad Shahidehpour (F'01) received the Honorary Doctorate from the Polytechnic University of Bucharest, Bucharest, Romania, in 2009. He is

the Bodine Chair Professor and the Director of Robert W. Galvin Center for Electricity Innovation at Illinois Institute of Technology, Chicago, IL, USA. He is a Research Professor with King Abdulaziz University, Jeddah, Saudi Arabia, and Sharif University, Tehran, Iran, as well as several universities in China including Tsinghua University, Beijing, North China Electric Power University, Beijing, Hunan University, Changsha, Xi'an Jiaotong University, Xi'an, and Southeast University, Nanjing. He was the recipient of the 2012 IEEE PES Outstanding Power Engineering Educator Award.

Ahmed Alabdulwahab (SM'13) received the Ph.D. degree in electrical engineering from the University of Saskatchewan, Saskatoon, SK, Canada. He is an Associate Professor with the Department of Electrical Engineering and Computer Engineering and affiliated with the Renewable Energy Research Group, King Abdulaziz University, Jeddah, Saudi Arabia. He has been a Consultant to the Electricity and Co-Generation Regulatory Authority in Saudi Arabia and a Visiting Scientist at Kinectrics, Etobicoke, ON, Canada, and the University of Manchester, Manchester, U.K. His research interests include power system planning and reliability evaluations..

Abdullah Abusorrah (SM'14) received the Ph.D. degree in electrical engineering from the University of Nottingham, Nottingham, U.K. He is an Associate Professor with the Department of Electrical Engineering and Computer Engineering, King Abdulaziz University, Jeddah, Saudi Arabia. He is the coordinator of the Renewable Energy Research Group and member of the Energy Center Foundation Committee at King Abdulaziz University. His research interests include power quality and system analyses.